19th Brazilian Congress of Thermal Sciences and Engineering
November 06th-10th, 2022, Bento Gonçalves - RS - Brazil

FLOW PATTERNS IN HORIZONTAL TRANSPORTATION OF BENTONITE PARTICLES

Yamid J. García-Blanco
Angel D. J. Rivera-Jiménez
Luis Quitian-Ardila
João Flórido
Eduardo Germer
Admilson Franco
Research Center for Rheology and Non-Newtonian Fluids – CERNN, Federal University of Technology-Paraná – UTFPR, R. Deputado Heitor Alencar Furtado, 5000 Curitiba, PR 81280-340, Brazil.

yamidblanco@alunos.utfpr.edu.br, angeljimenez@alunos.utfpr.edu.br, luis.2019@alunos.utfpr.edu.br, jflorido@alunos.utfpr.edu.br, eduardomg@utfpr.edu.br, admilson@utfpr.edu.br.

Abstract. *Offshore operations into the Oil & Gas explorations have grown during the last decade, especially in the Brazil's southeast coast. The massive extraction of petroleum reserves has dried at least one-third of all oil and gas wells, which has increased the Plugging & Abandonment (P&A) activities. Most of the abandonment activities are not checked and are assumed that the plug has been properly placed. This situation represents an environmental risk and has demanded properly P&A methodologies from many governments to the oil exploration companies. Bentonite particles have become in an alternative for P&A of oil wells. The bentonite works as an expansive clay that increases its size when it is in contact with water forming a plug. Bentonite plugs have shown to be safer, cleaner and environmentally friendly than the typical materials used for P&A activities, such as Portland cement. In the offshore scenario, the pumping of bentonite particles as a two-phase mixture with oily fluids represents a challenge, due to the vast quantities of particles that need to be displaced to a final target in order to accomplished the plugging process. Then, it is crucial to understand the solid-solid and solid-liquid interactions during the transportation of the bentonite particles to avoid excessive pressure losses and premature plugging along the pipeline. The main purpose of the present work is to study the flow patterns during the transportation of irregular bentonite particles in a horizontal pipe with oily Newtonian fluid. Solid glass beads of 4 mm with density of 2400 Kg/m^3 are utilized as bentonite particles. The formation of the different particle beds is visualized as a function of the flow regime and the pressure drop along a test section. The current results are performed following the same flow regimes, solid-liquid density ratio and geometrical aspect ratio from real field P&A conditions with bentonite particles transportation. The experimental results from the present work give previous interesting information about the mechanism and the interaction of the two-phase flow during the bentonite particle transportation, supporting with reliable data the execution of future planned P&A activities in offshore operations.*

Keywords: *Plug & Abandonment solutions, bentonite particles, flow patterns, solid-liquid interactions, pressure losses.*

1. INTRODUCTION

The plugging and abandonment process has received an especial attention from the Oil & Gas companies due to the material used for permanent plugging are subjected to different stress scenarios, such as tectonic stress and temperature changes (Khalifeh and Saasen, 2020). The Portland Cement has been the traditional material for permanent abandonment, nevertheless, there are some concerns about its long-term degradation. Therefore, some alternative plugging materials have been suggested, such as the bentonite, which is an expansive clay that expands its volume when contact with water. The bentonite expansion can reach up to 1000% its original size (Komine and Ogata, 1996; Barbosa et al., 2021); also, high level of adhesion with the well surface is depicted, which make the bentonite a suitable material for generating resistant particle agglomeration for well plugging.

The bentonite pellets are supply by the Brazilian manufacturer with cylindrical format, nevertheless is difficult to keep their geometrical integrity during transportation before the P&A activities. The latter leads to used non-uniform bentonite particles for the well plugging process. In the offshore scenario is required to pump the bentonite particles into long pipeline sections until the final destination, where the particles will act as a plugging barrier. Similar to cuttings

transportation during drilling activities, the bentonite particles transport in horizontal and directional wells for P&A process represents a challenge. This is because the particles tend to accumulate at the down wall due to gravity, forming stationary or moving beds (Luo and Peden., 1987; Barooah et al., 2022). One of major points for particles transporting and flow assurance is the prediction of the pressure drop. The existence of different phases and different operation parameter such as particle concentrations and pipe inclinations make difficult obtain a properly prediction of the pressure drop.

Different flow patterns can be encountered during the solids transportation, which depend on different parameters such as the fluid viscosity flow rate, the particle size and density, as also as the geometrical aspect ratio between the particles and the pipe or wellbore (Goharzadeh et al., 2008; Nossair et al., 2012). The Figure 1 illustrates the most common flow patterns encountered in particle transport. The first flow pattern is the bed load, where the flow velocity reaches the critical velocity to initiate particle movement and the particles move in a thin layer along the bed of particles, this pattern is known as rolling motion (Nossair et al., 2012). Below the critical Reynolds, the particles are deposited at the bottom of the pipe forming the stationary bed (Goharzadeh et al., 2008). The second flow pattern is the saltation motion. In this condition, the fluid flow velocity is higher than the critical velocity required to initiate the particle movement, but not sufficient to suspend the particles. In this pattern the particles are moving from downstream to upstream creating dunes forms (Nossair et al., 2012). The third flow pattern is known as suspension. In this pattern, the fluid flow velocity is capable to suspend the particles and a fully developed slurry mixture is obtained (Goharzadeh et al., 2008). Figure 1 presents the different flow patterns observed in experimental performances for solids transportation. According to Phillips (1980) and Corredor et al. (2016) higher critical velocity and pressure drop are required for initiating the rolling motion and after a change of pattern during the particle transportation is depicted as a change in the slope of the pressure drop as a function of the mean velocity.

Few works described by experimental performance the bed particle formation and the different motion patterns, and most of these experimental investigations are limited to a qualitative description and are compared with numerical results. Therefore, the present experimental work is addressed to visualize the bed particle formation and the possible development of bed patterns during the transportation of bentonite particles and their effects on the pressure drop along the pipeline.

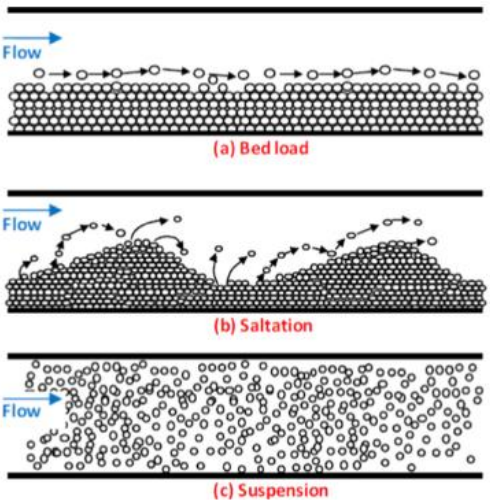

Figure 2. Flow patterns observed during particles transportation. Adapted from Goharzadeh et al. (2008).

2. EXPERIMENTAL SETUP

The current study is caried out in a flow loop of 16 m; a schematic diagram is shown in Figure 2. The test section (1) consists of transparent pipe of acrylic which provides optical access for flow visualization. The flow loop facility is an assembly of pipes with an internal diameter of D= 44 mm. Newtonian fluid (water) is contained in a 100 L tank (2) provided with a mixing system. The flow is pumped by a helical rotor mono pump of 5 HP (3), which is controlled by a frequency inverter with the aid of a mass flow meter (4); temperature and density are measured as outputs of the flow meter; the error mass flow meter upon the mean flow was estimated to be ± 0.1%. Pressure measurements are obtained by a differential pressure transmitter (5) place at the acrylic test section with a distance of the measurement points of 1 m. Pressure tappings (6) with 4 mm of internal diameter were connected to the pressure transmitter by cylindrical tubes filled with water to avoid the entrance of air and possible modifications in the pressure data. The pressure transmitter error is estimated to be ± 1% for a full measurement range, until 138 bar. The particles are injected before the acrylic test

section (7), at this point for the first tests the injection is manual assuring a fixed mass of particles that will be varied from 0.2 to 0.4 kg. The tests are performed with 4 mm glass beads into water as working fluid. The density of the glass beads is about 2400 Kg/m^3, this condition guarantees the same density ratio (ρ_s/ρ_f) presented during P&A with bentonite particles with oily fluid.

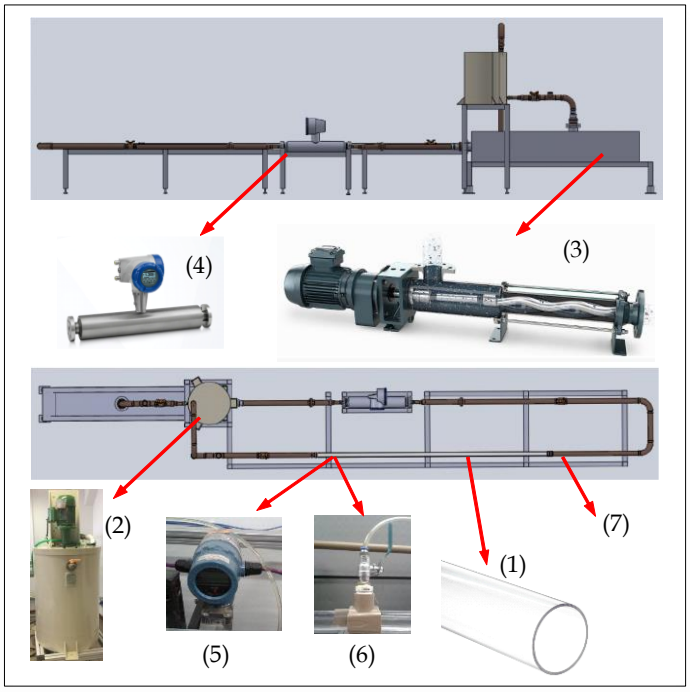

Figure 2. Experimental flow loop setup for tests performance

Table 2 presents the real field conditions for P&A operations; they are compared with the parameters set in the present experimental study. The geometrical ratio between the solid particles and the pipeline diameter were simulated, as the wall effects and the flow conditions are essential to represent the turbulent dynamic in the solid-liquid flow. In field condition the mean operational flow is around 29 bbl/min (barrel per minute), since the current experimental setup is limited to approximately 1.5 bbl/min the flow conditions are set by the Reynolds number with turbulent characteristic.

Table 2. Comparison of the real field operational data and the current experimental setup parameters. The real field density and geometrical ratio were simulated to guarantee the same wall effects and flow conditions.

	P&A real field conditions	**Current work**
Pipeline diameter (m)	0.114	0.044
Particle diameter (m)	0.01	0.004
Diameter ratio (-)	11.43	11
Operational Reynolds number (-)	30000-40000	10000-50000
Fluid density (Kg/m^3)	865	998
Solid particles density (Kg/m^3)	2200	2400
Density ratio (-)	2,54	2,4

Figure 3 presents a schema of the experimental array for visualization of the two-phase flow. This array consists of a monochrome high speed Chronos 1.4 camera from *Kron Technologies Inc* mounted in the flow loop structure with a back illumination system. The visualization plane of the camera is placed 90° to the pipe flow, the light scattering is reduced by the back light source that have and diffusor system. Possible distortion into the images is avoided by the similar refraction index of the acrylic and the water, close to 1.4. The typical frame rate used is 4000 FPS to record for a period of 16 seconds, enough for capturing the bed particle formation. The storage capacity of the camera is set to 32 GB which allows high-definition recording (1800 x 1024 pixels) in monochrome format.

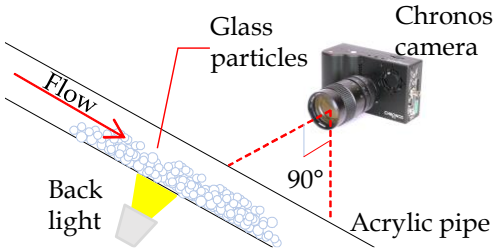

Figure 3. Experimental array for high-speed visualization

The pressure drop variation is also measured during the displacement of the particles along the test section. Figure 4 shows a schematic representation of the displacements of the glass beads during the performance of the experimental test. The glass beads flow like a packed body through flow loop, the pressure drop is measured when the particles flow between the measuring points *1* and *2* in order to obtain the pressure drop variations along the test section from a monophasic to a biphasic flow. The *F1* stage shows the condition when the amount particles reach the first pressure measured point *1*, afterwards the back tail of the particle pack reach the same measure point at the stage, and they are placed between the two measurement pressure points at the stage *B1*, in this condition the pressure drop correspond to a fully biphasic flow. Then, the front of the particles reaches the second point for the measurement of pressure drop at the stage *F2*, and dislocate until the back part of the group of particles get out from the pressure measurement region, at the *B2* stage where a monophasic flow is depicted again.

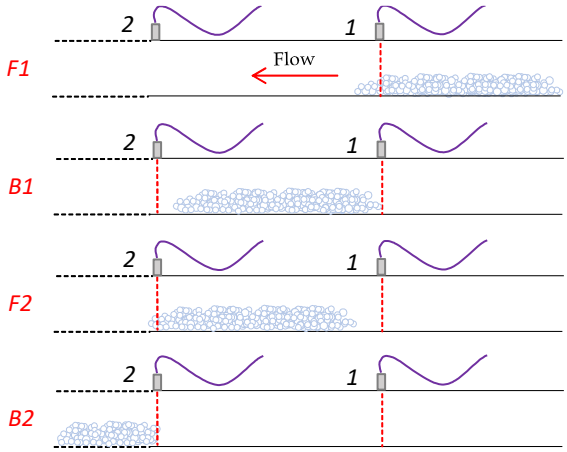

Figure 4. Glass beads flow along the test section. The particles flow in a pack through the pressure drop measure point, a variable pressure drop behavior is obtained as a consequence of the solid-liquid transportation.

3. PREVIOUS *f* vs *Re* VALIDATION TESTS

Previous tests were performed to assure a proper pressure drop measurement. In order to achieve this aim, Reynolds numbers between 9000 and 50000 were set using the classical Reynolds number definition for a single-phase flow

$$Re = \frac{\rho U D}{\mu} \tag{1}$$

where ρ is the fluid density, U the mean axial velocity along the pipe, D is the internal diameter and μ the dynamic viscosity of the fluid.

Figure 5 shows the f – Re graphic where the experimental data are compared with Blasius equation for turbulent Reynolds numbers. The Reynolds numbers were set to be turbulent due to the particle transportation is guarantee for this regime. The experimental friction factor was determined by $f = \frac{2\tau_w}{\rho U^2}$, where τ_w is the wall shear stress defined as $\tau_w = \frac{\Delta P D}{4L}$, and ΔP is the pressure drop over the length between the measurement points of the pressure transducer. Each experimental data was obtained from the pressure drop measurement during 60 seconds, due to the flow regime is turbulent it is necessary assure a good statistical density of the experimental data. Figure 3 shows good agreement of the experimental data with the Blasius equation $f = \frac{0.316}{Re^{0.5}}$. The errors bars show the standard deviation for each Reynolds

number set for this validation stage. For *Re* < 15000 there are more instabilities and greater standard deviation values because the pump system of the experimental flow loop starts the flow with a minimum *Re= 9000* for the currently experimental configuration, and some fluctuations can appear for low flow rates.

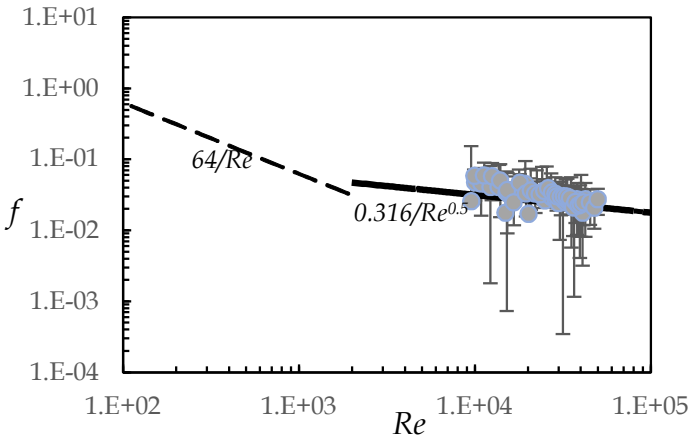

Figure 5. Friction factor and Reynolds correlation for Reynolds number between 9000 and 50000. Error bars depict the standard deviation of the values

4. RESULTS

4.1. Mean kinetic energy and flow patterns

The particle transportation is initiated after a critical velocity is reached; this is equal to a critical kinetic energy since the kinetic energy is directly dependent on the mean velocity of the flow. Figure 6 and 7 show the change of the flow pattern as a function of the kinetic energy at the entrance of the test section. The rolling motion is depicted for the low kinetic energy values, and then a saltation motion is presented after variations in the kinetic energy value. The mean kinetic energy is given by $K = \frac{1}{2}\rho_f U^2$, where U is the mean axial velocity at the entrance of the test section, and ρ_f the density of the fluid.

An abrupt transition of flow patterns is observed for both mass of particles. Such as behavior can explained the abrupt variation of the pressure drop slope presented in subsection 4.3. Critical kinetic energy values are then observed to lead the particles to a flow pattern change.

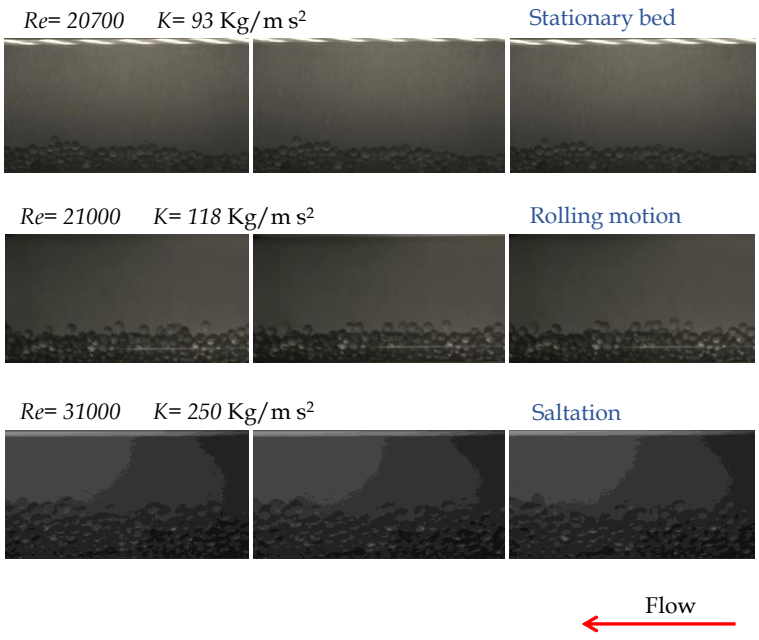

Figure 6. Flow pattern evolution as a function of the mean kinetic energy at the entrance of the test section for 200 gr of solid glass beads.

For the 400 gr case the particle seems to entrain in the saltation flow pattern with a low mean kinetic energy. This could be explained by the proximity of the particles to the central region of the pipe where higher velocity values are encountered. As the entrance flow at the test section is in turbulent conditions, high quantities of energy are encountered at the central region and this promotes an early change of conditions of the flow pattern for higher mass of particles. Nevertheless, further experimental tests are required to determine if this trend is presented for other amount of mass.

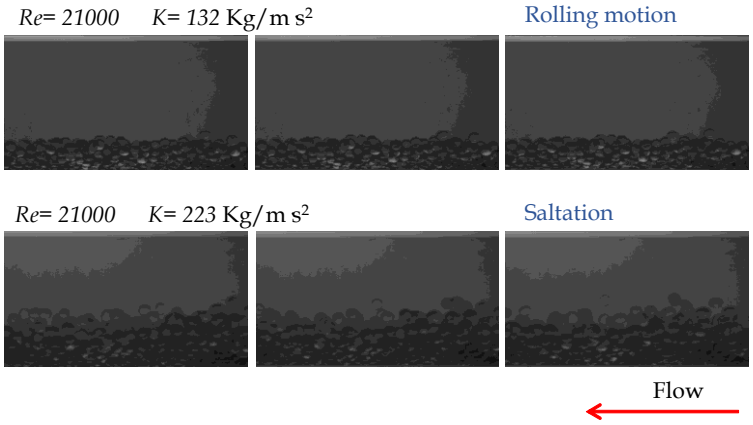

Figure 7. Flow pattern evolution as a function of the mean kinetic energy at the entrance of the test section for 400 gr of solid glass beads.

4.2. Transport efficiency

One of the main questions about the success of the P&A operations is the quantity of particles that can be placed at the target position. In real field configurations long pipelines with inclinations are used since the sea bed is not a regular surface; this can lead to critical regions with premature plugging. Therefore, the experimental setup was design with a final horizontal stage of 500D followed by a vertical line of 300D. At filter system was placed at the outer of the vertical line to retain the glass beads and obtain the mass transported by the flow. In order to determine the efficiency of the particle transportation, the solid-fluid flow was pumped during 180 s, thenceforth the particle collected at the filter system were weighed in a precision electronic balance and then the efficiency calculate as $E_T = \frac{m_c}{m_e}$, where m_c is the collected mass of glass beads into the filter system and m_e is the mass of beads entered to the flow loop. Figure 8 shows the particle transport efficiency for Reynolds number between 2000 and 35000 for different glass beads mass (200 gr and 400 gr). The transport efficiency is higher than 0.9 for both cases; nevertheless, a parabolic trend is depicted for 200 gr. On the other hand, for 400 gr the efficiency depicted a linear trend and the efficiency values are higher than the 200 gr case for the same *Re*. This behavior could be explained by the number of particles interacting in a similar volume fraction of the test section, since each 200 gr is equivalent approximately 3400 glass beads. An increase of the number of bodies interacting in a turbulent flow increase the turbulent kinetic energy of the solid-glass mixture and as a consequence the increase of the particle transport efficiency is provided by the solid-liquid interaction.

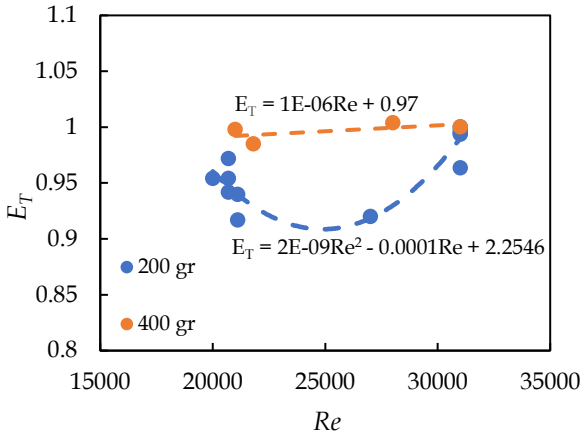

Figure 8. Particle transport efficiency as a function of the Reynolds number at the test section entrance.

4.3. Pressure drop slope and variation

As presented in Figure 4, the pressure drop was measured along the test section by a differential pressure transducer. A single case is evaluated in order to explain this topic in the present work, 200 gr of glass beads flowing with entrance Reynolds number of 21000, where a rolling motion is presented for these conditions. Figure 9 shows the evolution of the pressure drop along the four stages described in Section 2. The black lines depict the pressure drop oscillation for a turbulent single-phase flow and the mean pressure drop value which reach 56 Pa. The single-phase flow test was performed using the same *Re* at the entrance of the test section set for the biphasic flow with 200 gr of glass beads. After reach the *F1* stage the pressure drop increase with a quasi-linear trend until the *B1* stage, where the pressure drop reach a value between 150 and 180 Pa. After the *F2* is reached the pressure drop depicts a peak and decrease with a polynomial trend until the monophasic behavior is reached. Between the stages *B1* and *F2*, when the biphasic flow is completely consolidated in the test section, the pressure drops increased until three times the pressure drop value presented in the monophasic stage. The latter shows that pressure drop variation during the transportation of bentonite particles is an important parameter to be controlled for flow assurance in P&A activities.

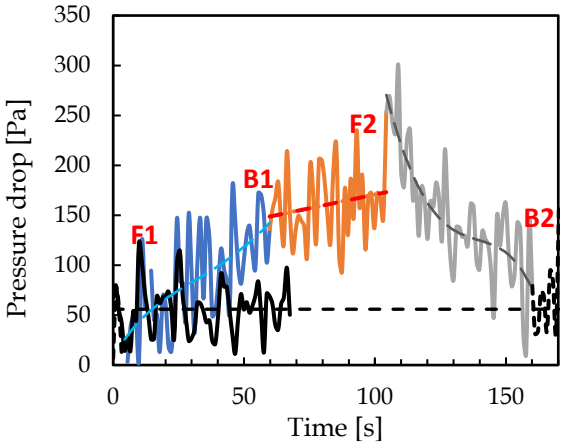

Figure 9. Pressure drop evolution along the test section during the particle transportation. The black lines show the trend for a single-phase flow.

The pressure drop during the *B1-F2* stage is depicted in Figure 10 for different Reynolds number for 200 gr and 400 gr of glass particles, also the pressure drop single-phase results are compared with results previously obtained in the validation tests. The pressure drop shows to be increased with the quantity of particle, due to for the single-phase case the pressure depicts values lower than 200 Pa for the range of Reynolds number performed. Also, the pressure drops increase with the Reynolds number for the same mass of particles and change in the slope is presented in *Re*=31000 for 200 gr of particles, and *Re*=24000 for 400 gr. Such as behavior is presented by Corredor et al. (2016), where an increase of the pressure drop with the *Re* was also depicted, and the change of the slope was related with the change in the flow pattern, that means a transition between the different modes of solids transport.

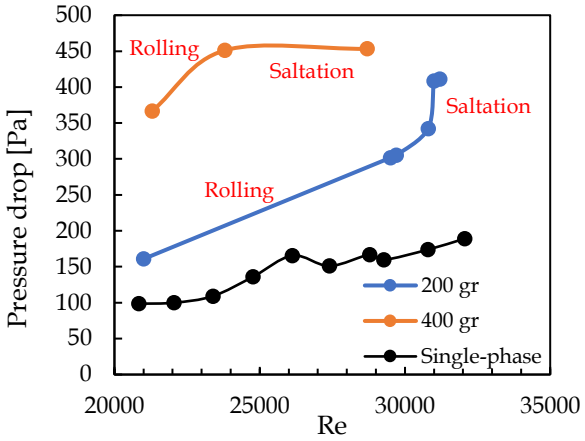

Figure 10. Pressure drop evolution along the test section during the particle transportation. The black lines show the trend for a single-phase flow.

The changes in the pressure drop slopes indicates that for a higher amount of particle the change of pattern is early reached when the increase of the Reynolds number. This could be explained by the quantity of particles that are placed near to the central region of the pipe, where the axial velocity reaches the maximum value. It is necessary more experimental test to obtain a detailed pressure drop plot and compare the results in a wider range of Reynolds numbers. Nevertheless, for the Reynolds numbers compatible with the conditions of the real field for P&A activities a good description of the flow patterns and the differences with a single-phase flow is obtained, providing reliable data for abandonment operations.

5. CONCLUSIONS

The particle transportation tests show the importance of the mechanism for the flow pattern formation and the change of these pattern as a function of the changes in the flow regime. Pressure fluctuations are depicted during the particle transportations due to the movement of the particles, since the motion started with a rolling pattern and then changes to a saltation motion as the Reynolds number is increased. Also, higher pressure drop is depicted for flows with solid particles when compared with single-phase flow, this behavior is presented by the perturbations generated by the motion of the particles. Therefore, higher amount (mass) of particles leads to a higher pressure drop. Changes in the trend of the pressure drop has a direct relationship with the change of the flow pattern such as the perturbations generate by the particle motion is increased and is reflected by pressure losses.

To initiate the particle motion after a bed load formation it is necessary to exceed a critical velocity or in terms of energy, a critical kinetic energy. The motion is then initiate instantaneously after the critical kinetic is reached and the efficiency is by far quite acceptable for low energy requirements after the motion has been initiated. Transport efficiency of 90% is depicted for the initial cases where was detected particle transportation.

Finally, these results show different parameters to be considerate for the transportation of bentonite pellets for P&A activities. An acceptable particle displacement is obtained for low energy requirements and pressure drop. Despite the mass of particles is increased, the transport efficiency reaches a constant value and seems to be invariable at least for the operational Reynolds numbers required for the P&A process studied in the present work.

6. ACKNOWLEDGEMENTS

This study was financed in part by the Coordination for the improvement of Higher Education Personnel – Brazil (CAPES)- Finance Code 001. The authors also would like to thank the financial support of the Brazilian National Council for Scientific and Technological Development (CNPq).

7. REFERENCES

Barbosa, F. T., Lugarini, A., García-Blanco, Y., Germer, E. M., & Franco, A. T., 2021. “Contact properties and modelling of bentonite pellets displacement for plugging and abandonment in offshore oil wells”. In *Proceedings of the 26th Internacional Congress of Mechanical Engineering – COBEM 2021*. Florianopolis, Brazil.

Barooah, A., Khan, M. S., Khaled, M. S., Rahman, M. A., Hassan, I., Hasan, R., Maheshwari P. & Hascakir, B., 2022. “Investigation of cutting transport in horizontal/deviated annulus using visualization and pressure drop techniques for two-phase slurry flow”. *Journal of Natural Gas Science and Engineering*, vol. 100, p. 104460.

Corredor, F. E. R., Bizhani, M., & Kuru, E., 2016. "Experimental investigation of cuttings bed erosion in horizontal wells using water and drag reducing fluids". *Journal of Petroleum Science and Engineering*, 147, 129-142.

Goharzadeh, A., Rodgers, P., Touati, C., 2008. "Influence of slug flow on hydraulic sand dune migration in horizontal pipelines". In *Proceedings of ASME 2008 International Mechanical Engineering Congress & Exposition*. Boston, Massachusetts, USA.

Komine, H., Ogata, N, 1996. "Prediction for swelling characteristics of compacted bentonite". *Canadian Geotechnical Journal*, Vol. 33.

Khalifeh, M. and Saasen, A., 2020. *Introduction to permanent plug and abandonment of wells*. Springer Nature, Cham, Switzerland, Volume 12.

Luo, Y., and J. M. Peden., 1987. "Flow of drilling fluids through eccentric annuli". In *SPE 16692 -62nd Annual Technical Conference and Exhibition*, Dallas, USA.

Nossair, A. M., Rodgers, P., & Goharzadeh, A., 2012. "Influence of pipeline inclination on hydraulic conveying of sand particles". In *ASME International Mechanical Engineering Congress and Exposition (Vol. 45233, pp. 2287-2293)*. American Society of Mechanical Engineers. Houston, Texas - USA

Zheng, E., Rudman, M., Kuang, S., & Chryss, A., 2021. "Turbulent coarse-particle non-Newtonian suspension flow in a pipe". *International Journal of Multiphase Flow*, Vol. 142, p. 103698.

8. RESPONSIBILITY NOTICE

The author(s) is (are) the only responsible for the printed material included in this paper.